



Synthesis of 5-hydroxymethylfurfural and furfural in 1,4-dioxane versus acetone: Comparing reaction performance and solvent recyclability parameters

David Cruz^{a,1}, Hyeonji Park^{a,2}, Phoenix Tiller^{a,3}, Ronalds Gonzalez^{a,4}, Ashutosh Mittal^{b,5}, David K. Johnson^{b,6}, Sunkyu Park^{a,*,7}

^a Department of Forest Biomaterials, North Carolina State University, Raleigh, NC 27695, USA

^b Renewable Resources and Enabling Sciences Center, National Renewable Energy Laboratory, Golden, CO 80401, USA

ARTICLE INFO

Keywords:

Biorefinery
Bioeconomy
Process design
Solvent recovery
Azeotrope
Heat duty

ABSTRACT

Research on monosaccharide dehydration primarily focuses on combining catalysts and organic solvents to maximize product yields. This study evaluates reaction performance and solvent recyclability experimentally and through process simulation, emphasizing their role in biorefinery design. Glucose and xylose, at intermediate aqueous sugar concentration, were dehydrated over aluminum chloride using 1,4-dioxane or acetone as co-solvents. Both organic systems exhibited comparable results, with 100 % sugar conversion. The 5-hydroxymethylfurfural yield reached 60.9 ± 0.2 % for 1,4-dioxane and 59.5 ± 0.6 % for acetone systems, while the furfural yield reached 78.1 ± 0.8 % and 78.9 ± 1.5 %, respectively. Process simulations indicate that using acetone instead of 1,4-dioxane can significantly reduce heat duty during the solvent recovery stage by 72 %, solvent loss by 60 %, and catalyst loss by 48 %. A multi-stage continuous distillation system was built to recover solvents from model solutions. The results highlight the advantages of using acetone instead of 1,4-dioxane, offering insights for improving energy efficiency in biorefinery processes.

1. Introduction

The abundant carbon-rich lignocellulosic biomass is a promising alternative feedstock to the fossil-based economy for producing high-value-added products such as polymers, solvents, syngas, liquid fuels, etc. [1]. Glucose and xylose are the primary monomeric products after the complete saccharification of cellulose and hemicellulose, present in lignocellulosic biomass. These monosaccharides can be upgraded under acidic conditions to 5-hydroxymethylfurfural (5-HMF) and furfuraldehyde (furfural), respectively [2]. The U.S. Department of Energy has

identified these 5-HMF and furfural as key bio-based C5 and C6 precursor platforms for decarbonizing global economies [3].

5-HMF and furfural have been utilized at the laboratory scale as starting materials to produce various molecules through different conversion strategies, including aldol-condensation, decarbonylation, decarboxylation, hydrogenation, oxidation, etc. [4]. From an economically significant perspective, 5-HMF can yield 2,5-furandicarboxylic acid (FDCA), the precursor of polyethylene furanoate (PEF), a 100 % bio-based polymer with the potential to replace polyethylene terephthalate (PET), the second most used polymer worldwide, with an

* Correspondence to: Jordan Family Distinguished Professor and University Faculty Scholar, Department of Forest Biomaterials, NC State University, Biltmore Hall Campus Box 8005, Raleigh, NC 27695-8005, USA.

E-mail addresses: cdcruzri@ncsu.edu (D. Cruz), hpark22@ncsu.edu (H. Park), ptiller@ncsu.edu (P. Tiller), rwgonzal@ncsu.edu (R. Gonzalez), ashutosh.mittal@nrel.gov (A. Mittal), david.johnson@nrel.gov (D.K. Johnson), sunkyu_park@ncsu.edu (S. Park).

¹ ORCID: 0000-0001-8909-6157

² ORCID: 0000-0002-3890-6348

³ ORCID: 0009-0003-8396-1017

⁴ ORCID: 0000-0001-5282-3015

⁵ ORCID: 0000-0002-0434-0745

⁶ ORCID: 0000-0003-4815-8782

⁷ ORCID: 0000-0002-9332-9061

estimated annual global market value of USD 44.1 billion in 2020 [5]. Likewise, more than 80 different chemicals can be synthesized from furfural, a material with a market size of USD 520 million in 2021 [5,6].

The saccharification of polymeric carbohydrates in lignocellulosic biomass to monomeric sugars typically involves significant amounts of water in both enzymatic and nonenzymatic processes (e.g., acid hydrolysis) [7]. Low-solids biomass loadings (5 wt%) yield over 80 % carbohydrate conversion [8], while high-solid loadings (15 wt% – 35 wt %) significantly reduce conversion to below 60 % [9]. Consequently, this process often results in highly diluted sugar products, which impacts biorefinery capital and operational costs. Therefore, understanding the transformation of monomeric carbohydrates into furanic compounds in intermediate to high sugar-content systems is crucial for industrial applications.

During the acid-catalyzed dehydration of glucose and xylose in aqueous systems, the addition of an organic co-solvent, such as DMSO, 1,4-dioxane, 1-butanol, MIBK, THF, etc., has been used to enhance the yield of 5-HMF and furfural by reducing unwanted side reactions, including nucleophilic addition, self-condensation, and polymerization leading to humin, a dark-colored polymeric network of furanic derivatives that is known for its ability to block reactors, deactivate catalysts, and absorb high-value molecule products [5,10,11]. The use of organic solvents forming a biphasic system with the aqueous sugar solution, along with the addition of modifiers aimed at enhancing phase separation and promoting the migration of furanic compounds to the organic phase, has been widely adopted in recent years. However, the high amount of required modifier and its chemical nature (e.g., 20 wt% - 35 wt% NaCl) can be detrimental to the process's economy due to the need for additional separation units, increased wastewater treatment cost, and the requirement for specialized equipment materials [12]. Additionally, the biphasic approach is often oversimplified by suggesting single decanting units to separate the dehydration products in the organic phase, ignoring the solvent loss in the aqueous phase, which can be economically restrictive [13].

Biorefineries are expected to operate sustainably [14]. Therefore, a thorough analysis is required during their conceptual design [15]. Continuous distillation has been used to recover organic solvents during the production and purification of bioethanol, lactic acid, 5-HMF, and furfural [16]. Several physicochemical properties can affect the operation of distillation columns, such as the presence of solid materials, the instability of the processed components, and the occurrence of azeotropic nodes between the chemicals of interest, among others [17].

High carbohydrate conversion rates (92 % - 100 %) and yields of furans (75 % - 80 %) have been documented when 1,4-dioxane is used at high organic solvent-to-aqueous volume ratios (e.g., 5–1) during the dehydration reaction of monomeric sugars (6 wt% aqueous sugar content) over Lewis-acid catalysts [18]. This solvent has been recognized as one of the most effective organic solvents supporting glucose dehydration, based on both experimental and computational approaches [19]. These remarkable findings suggest that 1,4-dioxane may be suitable for producing C5 and C6 furanic compounds in industrial-scale applications. However, this aprotic solvent exhibits an azeotrope node with water under atmospheric conditions (82 wt% & 87.6 °C) [20,21]. This thermodynamic restriction adds complexity to its further separation and recovery. Furthermore, this solvent has been associated with potential genotoxic and harmful biological effects on rodents and other model organisms after chronic high-dose exposure [22]. Hence, finding an alternative solvent for designing an operationally safe, energy-efficient, scalable, and economically feasible process to produce large amounts of furans from lignocellulosic feedstocks is imperative.

This study aims to compare reaction performance and solvent recyclability parameters, both experimentally and through process simulation, during the dehydration of glucose and xylose at intermediate aqueous concentrations over aluminum chloride in miscible single-phase organic systems using 1,4-dioxane versus acetone to produce 5-HMF and furfural. Process models based on experimental dehydration

results are used to estimate process parameters such as recovered solvent purity, organic solvent loss, dehydration catalyst makeup, and heat duty across the reactor and the distillation unit. Furthermore, a multi-stage distillation system was built based on simulation results to analyze the distilled and heavy products for solvent and furanic compounds content. This study examines the production of 5-HMF and furfural, as well as the solvent recovery stage, as intermediate steps within a broader biorefinery process. It does not address the upstream transformation of biomass into sugars, further downstream purification and transformation of products, or waste stream treatment.

2. Materials and methods

2.1. Chemicals

Analytical reagents including D(+)-glucose (anhydrous, 99 %, Thermo Scientific™), D(+)-Xylose (>99 %, Thermo Scientific™), Aluminum Chloride (Hexahydrate, 99 %, Thermo Scientific™), 5-Hydroxymethylfurfural (≥99 %, Sigma Aldrich®), 2-Furaldehyde (99 %, Sigma Aldrich®), acetone (>99.5 %, Thermo Scientific™), 1,4-dioxane (99.5 %, Thermo Scientific™), Certified Reference Material for the quantification of glucose, xylose, 5-Hydroxymethylfurfural, and furfural (Absolute Standards, Inc), were used as received. Ultra-filtrated water (Milli-Q® Biocel water system) was utilized in all experiments.

2.2. Dehydration of monomeric sugars

A sugar solution was prepared using glucose, xylose, and ultra-filtrated water. An intermediate total sugar mass content of 20 wt% and a glucose-to-xylose mass ratio of 3.6–1, as typically found in lignocellulose-derived hydrolysate [23] and consistent with previous work by this research group on paper sludge hydrolysis [24]. The sugar dehydration experiments employed a volume ratio of organic solvent-to-aqueous sugar solution of 2–1. Five samples containing 1, 4-dioxane and five samples containing acetone were studied. Aluminum chloride (AlCl₃), a Lewis acid catalyst, was used at a total catalyst loading of 15 millimolar (mM) in the experiments according to the reaction pathways displayed in Fig. 1 [25–28]. Dehydration experiments were conducted using a CEM Discover 2.0 Microwave Synthesizer (CEM Corporation, Charlotte, NC) and 10 ml Pyrex vessels (maximum working pressure: 3000 kPa). A dynamic control method was applied for experiments, which allows the power to be automatically adjusted based on temperature and pressure sensor feedback, ensuring that the temperature control point was reached rapidly while minimizing temperature and pressure overshoot (maximum applied power: 300 W). After the setpoint temperature was reached, power consumption was measured at 155 W for 1,4-dioxane systems and 210 W for acetone systems (Supplementary material). A method was implemented with a setpoint temperature of 185 °C, which was determined as optimal based on previous experimental results for glucose dehydration (Supplementary material). Additionally, 15 seconds of pre-stirring, continuous stirring at a medium level, and a holding time of 3 minutes were applied. The typical ramping time was recorded at 2.5 minutes for 1,4-dioxane systems and 3.2 minutes for acetone systems. The quantification of unreacted sugars, as well as the produced furans, was carried out according to NREL procedures [29], using an Agilent HPLC 1260 equipped with a Bio-Rad, Aminex HPX-87H Organic Acid Analysis chromatographic column, a Diode Array Detector (5-HMF at 284 nm and furfural at 277 nm), and a Refractive Index Detector (Agilent Technologies, Santa Clara, CA). The conversions of glucose and xylose, as well as the yields of 5-HMF and furfural, were estimated using Eqs. (1) and (2).

$$\text{Sugar conversion}(\%) = \frac{\text{sugar consumed}(g)}{\text{sugar input}(g)} \times 100 \quad (1)$$

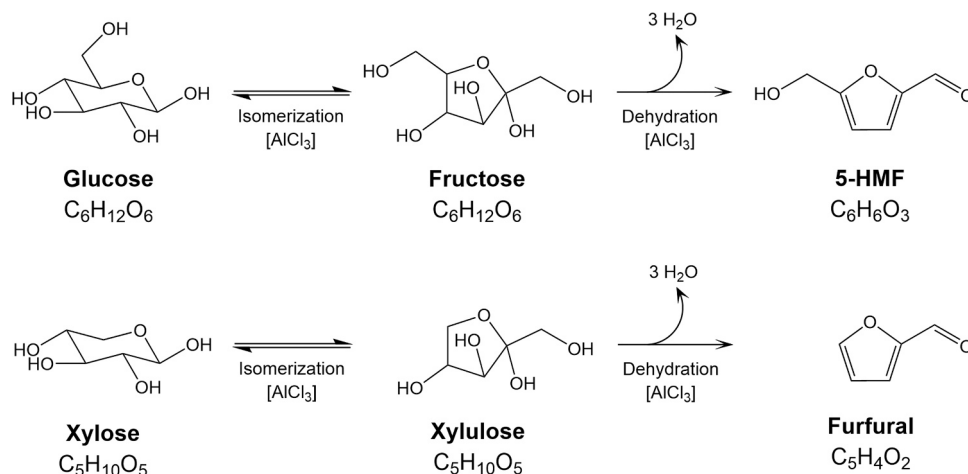


Fig. 1. Reaction pathways for the dehydration of glucose and xylose to 5-HMF and furfural, respectively, using aluminum chloride as a Lewis acid catalyst.

$$\text{Furanic compound yield}(\%) = \frac{\text{Furanic compound formed}(g)}{\text{Maximum possible furanic compound}(g)} \times 100 \quad (2)$$

2.3. Process description and process modeling

Previous studies on the recovery and reuse of miscible organic solvents used in sugar dehydration in hypothetical biorefineries suggested employing a single-stage evaporator [30,31]. However, this approach does not meet the requirement to separate the solvents to a high purity before recirculation. Therefore, a multi-stage distillation unit was employed in this work. The two-step biorefinery process flow diagram for the dehydration of glucose and xylose, along with the solvent recovery strategy, is depicted in Fig. 2. An aqueous sugar solution enters the mixer, combining with fresh organic solvent (1,4-dioxane or acetone), the catalyst supporting the dehydration reaction (aluminum chloride, $AlCl_3$), and a recycled stream primarily containing recirculated solvent. The mixture then flows into the dehydration reactor operating at 185 °C before being transferred to a continuous distillation system to separate and recirculate the organic solvent back to the mixer. Given the

complexity of the transport phenomena occurring in the distillation column, adequate process simulation software was required to estimate the heat demand across the process accurately. Aspen Plus™ (version 11) was employed to assess the mass balance and the thermal energy demand (heat duty) across the units shown in Fig. 2. The main set of equations used to solve the mass and energy balances across the biorefineries is available in the Supplementary material. Aspen Plus™ (version 11) has been validated in modeling modern biorefineries handling biomass conversion to sugars, furans, etc. [32]. In the simulation, sugars and solvents were considered “conventional materials,” and humin was handled as unreacted sugars, given the broad distribution of polymeric species forming this side product and the lack of detailed thermodynamic properties. Experimental results from the dehydration reaction were used to parameterize the reaction simulation block (e.g., operating pressure, conversion, yield). A distillation unit operating under atmospheric conditions with a typical reflux rate of 1.5 was used in the model. The total number of equilibrium stages and the “Feed stage” location were varied to minimize the reboiler heat duty.

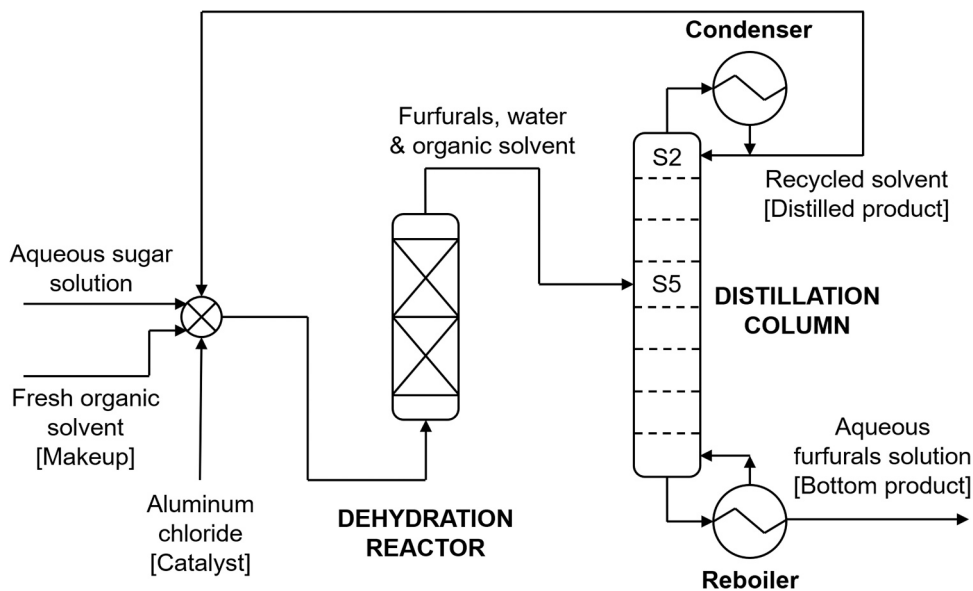


Fig. 2. Two-step biorefinery process flow diagram featuring a dehydration reactor and a distillation system to recover and recirculate the organic solvent after the reaction step.

2.4. Continuous distillation of organic solvents

To study organic solvent recovery from the dehydration product solution via bench-scale distillation, commercially available 5-HMF and furfural were used to prepare 300 ml of aqueous model solutions based on the findings from the dehydration experiment for each solvent system. Glucose and xylose were added in corresponding proportions to simulate the presence of humin and other side products. A corresponding volume of organic solvent (1,4-dioxane or acetone) was added at an organic solvent-to-aqueous solution volume ratio of 2–1. Using simulation data on theoretical equilibrium stages and the optimal “Feed stage” location, a multi-stage continuous distillation system was built to recover each solvent from the studied solutions (Supplementary material). Two six-section Snyder columns (ACE Glass Inc., Vineland, NJ), a 500 ml round-bottom flask serving as the reboiler, and a Graham condenser were assembled to create a system with fourteen equilibrium stages. A heating mantle with a magnetic stirrer (Fisherbrand™) was used as the heat source for the reboiler. This in-house-built distillation apparatus used two peristaltic pumps (Golander LLC, USA). The first pump transferred the furans solution containing organic solvent to “Equilibrium stage No. 8” (top to bottom). The second pump removed the bottom product from the round-bottom flask. Two temperature controllers (J-Kem Scientific Inc., St. Louis, MO) were utilized. The first controlled the temperature inside the reboiler at a setpoint of 101 °C. The second controller regulated the temperature of a heating tape wrapped around the distillation column to prevent heat loss to the

surroundings (room temperature: 20 °C). Its setpoint was set 2 °C below the expected distillate temperature reported in the literature for each solvent system: 87.6 °C (1,4-dioxane/water azeotropic mix) [20,21] and 56 °C (pure acetone) [33]. A reflux distillation splitter adapter (Chess Life Sciences LLC, Vineland, NJ) installed on top of the column assembly and below a glass spiral reflux condenser (Equilibrium stage No.1) was used to divert the recovered solvent (distilled product). Lastly, a local temperature indicator (Sper Scientific LLC, Scottsdale, AZ) was installed at “Equilibrium stage No. 2” to measure and record the temperature in this section. The quantification of 1,4-dioxane and acetone at the distillate and bottom products was carried out using an Agilent HPLC 1220 equipped with an InfinityLab Poroshell 120 EC-C18, 4.6 mm x 100 mm and 2.7 μm chromatographic column, and a Variable Wavelength Detector at 190 nm and 266 nm respectively (Agilent Technologies, Santa Clara, CA).

3. Results and discussion

3.1. Microwave-assisted sugar dehydration reaction

The benefits of processing biomass at intermediate and high solids content on the overall economics during the production of bio-based chemicals and fuels in biorefineries have been widely supported [34, 35]. In this section, the dehydration of purchased glucose and xylose at an intermediate solids content of 20 wt% and a solvent-to-aqueous sugar solution volume ratio of 2–1 was investigated. The results for the

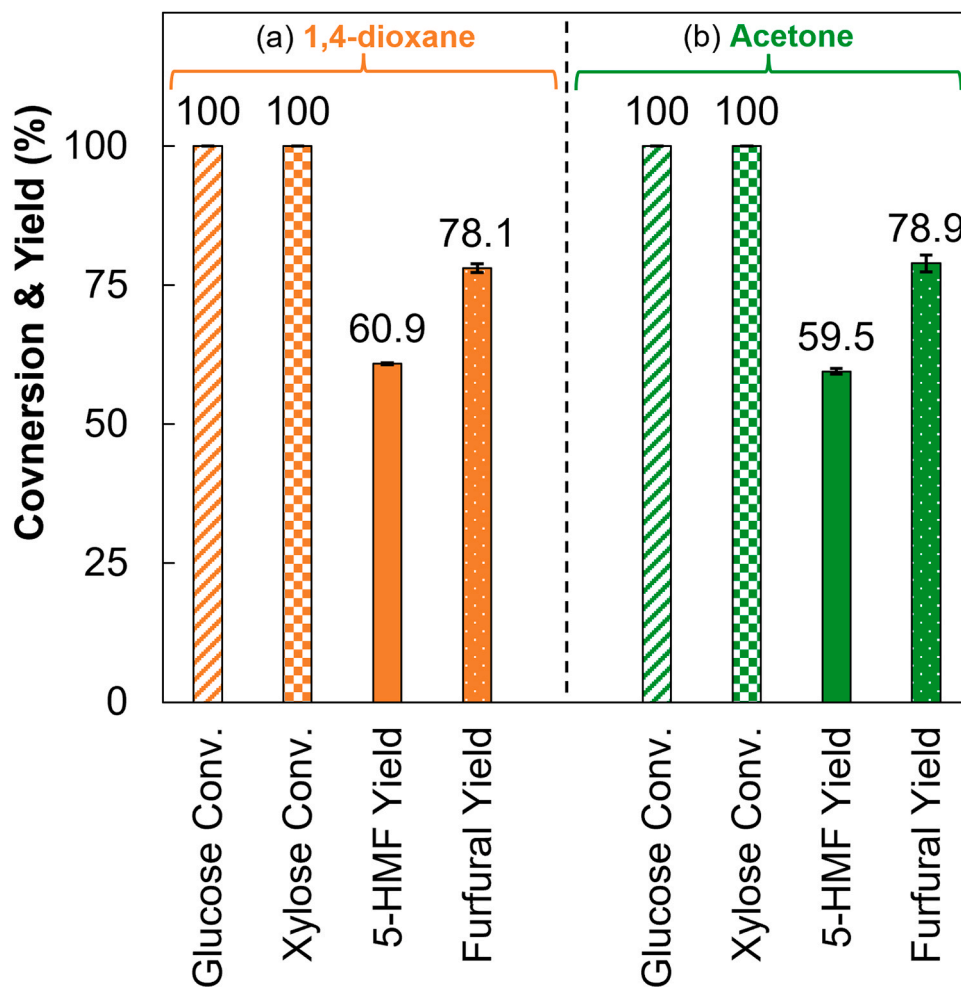


Fig. 3. Glucose and xylose conversion and yield of 5-HMF and furfural for (a) 1,4-dioxane and (b) acetone systems. Experimental conditions: 20 wt% total sugar aqueous solution, a glucose-to-xylose mass ratio of 3.6–1, 15 mM of AlCl₃, an organic solvent-to-aqueous sugar solution volume ratio of 2–1, setpoint temperature 185 °C, and a holding reaction time of 3 minutes.

conversion of sugars and the yield of furanic compounds during the dehydration reaction in 1,4-dioxane and acetone systems are displayed in Fig. 3. Both solvents exhibited comparable results, with 100 % conversion of sugars. The complete conversion of glucose and xylose achieved within the short reaction time in a CEM Discover 2.0 Microwave Synthesizer contrasts with the results of other reactor technologies (e.g., hydrothermal batch reactors) [31]. The yield of 5-HMF reached $60.9 \pm 0.2 \%$ for the 1,4-dioxane system and $59.5 \pm 0.6 \%$ for the acetone system, while the yield of furfural reached $78.1 \pm 0.8 \%$ and $78.9 \pm 1.5 \%$, respectively. These results are in agreement with previous studies utilizing aluminum chloride as a Lewis acid catalyst and aqueous solutions of sugars with lower solids content (5 wt%) and a higher organic solvent volume ratio (4–1, and 8–1) [26]. The reduction in the pH of the solutions after the dehydration reaction was observed at a consistent level (from pH 2.9 to approximately pH 1.9 at 21 °C) for both analyzed solvent systems (Supplementary material). This result has been previously explained as a consequence of side product formation, including levulinic acid and formic acid, arising from the degradation of 5-HMF and furfural [26]. The findings suggest that, under the investigated reaction conditions, replacing 1,4-dioxane with acetone has a negligible impact on the yield of the intended dehydration products.

3.2. Process simulation results

3.2.1. Thermodynamic model validation

Selecting an appropriate thermodynamic method and binary interaction parameter sources is crucial in process simulation to accurately represent experimental results for the systems under investigation. According to the literature, the Non-random Two Liquid (NRTL) thermodynamic method [36] closely reproduces experimental data for sugar dehydration and other biomass transformation operations [37]. Various thermodynamic methods and binary interaction parameter sources were evaluated using Aspen Plus™ (version 11) to identify the best set of equations to accurately represent experimental vapor-liquid equilibrium data reported in the literature for the analyzed organic solvent systems. After comparing the simulation and experimental results, the NRTL-2 property method with the binary interaction parameter sources APV110 VLE-IG and NISTV110 NIST-IG were selected for the process simulation work. The composition of the liquid and the vapor phases in equilibrium predicted by Aspen Plus™ (version 11) for the binary 1, 4-dioxane/water, acetone/water, and acetone/furfural systems at 101.325 kPa, along with experimental results from the literature, are presented in Fig. 4 and Supplementary material [20,21,33,38–40]. Theoretically, the azeotrope at high proportions of 1,4-dioxane and the “pinch” at high concentrations of acetone (Fig. 4) in aqueous systems may shift when reduced operational pressure is used (e.g., 10 kPa),

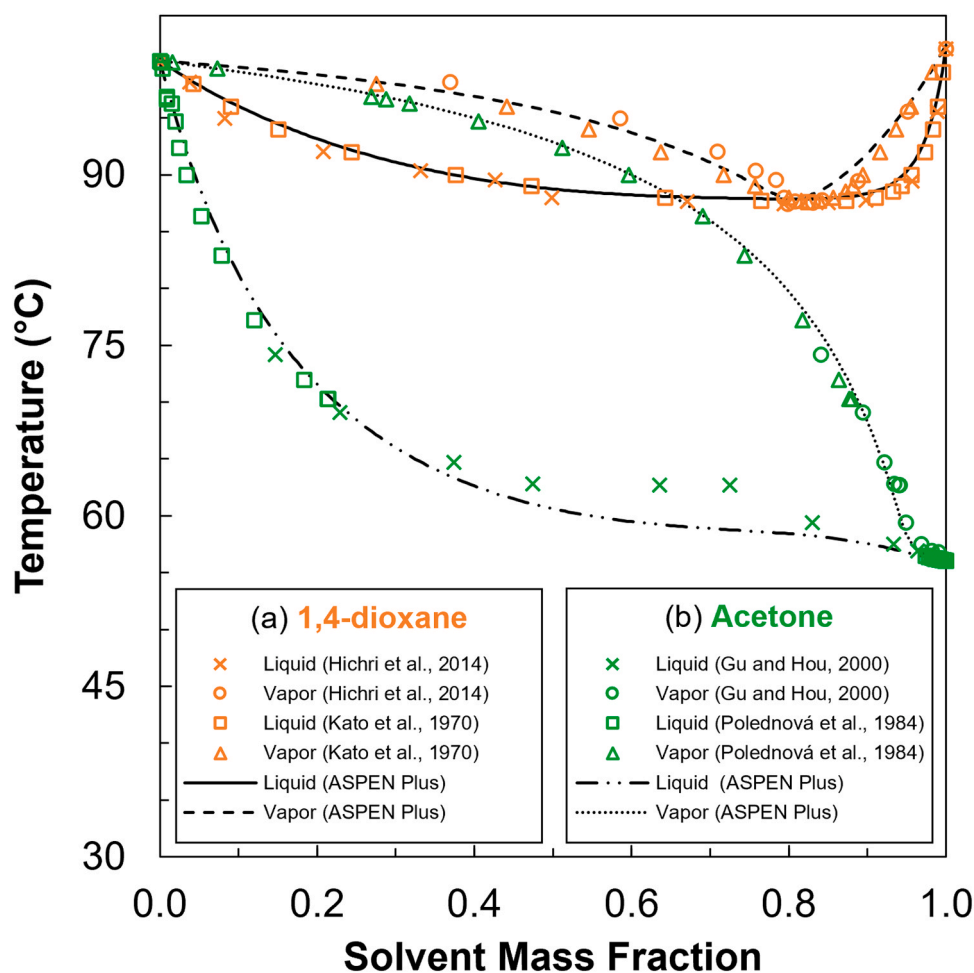


Fig. 4. (a) T-x-y diagram for 1,4-dioxane + water system: X_{orange} , T-x and \circ_{orange} , T-y for experimental data at 101.325 kPa [21]; \square_{orange} , T-x and Δ_{orange} , T-y for experimental data at 101.325 kPa [20]; —, T-x and —, T-y ASPEN Plus™ (NRTL-2 & APV110 VLE-IG) at 101.325 kPa. (b) T-x-y diagram for the acetone + water system: X_{green} , T-x and \circ_{green} , T-y for experimental data at 101.3 kPa [33]; \square_{green} , T-x and Δ_{green} , T-y for experimental data at 101.325 kPa [38]; - • • -, T-x and ••••, T-y ASPEN Plus™ NRTL-2 & APV110 VLE-IG) at 101.325 kPa.

(a) Reprinted with permission from Copyright© 2024 American Chemical Society & Taylor & Francis Ltd. (b) Reprinted with permission from Copyright© 2024 American Chemical Society & Elsevier.

potentially increasing the purity of the top product and lowering the heat demand at the reboiler. However, the experimental equipment available for comparison purposes operates at atmospheric pressure. Thus, this condition is used in the simulation work.

3.2.2. Biorefinery approach

Four different scenarios are analyzed, two for each solvent system: the “realistic” (closed) scenarios, where the solvent is distilled and recirculated to a mixing unit before reentering the dehydration reactor (Fig. 2), and the “non-realistic” (open) scenarios, where the solvent passes through the reaction and the distillation column only once, similarly to what can be replicated at bench scale. The results from the “open” scenarios are irrelevant for real industrial settings. Still, they are suitable for comparison with experimental distillation outcomes and useful for understanding the reason for the increase in total mass flow running through the distillation column, particularly in 1,4-dioxane systems, where a high proportion of water is recirculated.

The size of the hypothetical biorefinery is fixed at a processing capacity of 100 kg/h of sugars (500 kg/hr of 20 wt% sugar aqueous solution). The dehydration experiment results in Fig. 3, and the experimental operating pressure in the dehydration reactor (1,4-dioxane: 1634 kPa; Acetone: 2068 kPa) were incorporated as input data in the simulation models. Table 1 presents detailed results for the mass balance and the heat duty across the reactor and the distillation system for all cases after determining the optimal total number of equilibrium stages and “Feed stage” location for the analyzed solvent systems.

3.2.3. Solvent purity in distillate product

The simulation model predicts a mass percentage of 1,4-dioxane and the temperature in the distillate stream, closely matching the values reported in the literature (Simulation: 80 wt% and 88.0 °C; Literature: 82 wt% and 87.6 °C) [20,21]. Similarly, it suggests the possibility of distilling high-purity acetone (>98 wt%) at a temperature near the boiling point of pure organic solvent under atmospheric conditions (Simulation: 56.4 °C; Literature: 56 °C) [33], consistent with the “pinch” observed at high acetone concentrations (Fig. 4).

3.2.4. Organic solvent makeup

Due to the estimated ~20 wt% water content in the distillate stream being recirculated in the “realistic” 1,4-dioxane scenario, the amount of organic solvent entering the dehydration system needs to be increased by 98.5 % compared to its corresponding “non-realistic” model to maintain an organic solvent-to-aqueous sugar solution volume ratio of 2–1. Since the loss of organic solvent has been fixed at a typical industrial value of 2 % of the total solvent entering the distillation system [41, 42], the makeup of organic solvent in the “realistic” 1,4-dioxane scenario is also adversely affected (Table 1). Furthermore, an increased mass flow may also lead to higher capital expenditure due to the need for larger equipment. Conversely, the lower amount of water in the recirculated acetone (~2 %) predicted for the corresponding “realistic” acetone scenario leads to a 4.1 % increase in the solvent mass flow required to enter the reactor compared to its corresponding “non-realistic” scenario. This minor difference explains the similar results for the estimated mass balance and heat duty when comparing the “open” and “closed” models handling acetone (Table 1).

When comparing the results for the “realistic” scenarios of 1,4-dioxane and acetone systems, a fresh organic solvent makeup of 32.8 kg/hr is projected when using the cyclic ether. In contrast, the simulation predicts a lower makeup flow of 13.2 kg/hr if the volatile ketone is used. Based on the simulation results and under the assumptions made, substituting 1,4-dioxane with acetone yields a 60 % reduction in organic solvent loss, which could lead to lower operational costs considering the solvent price: USD 1300 per metric ton of 1,4-dioxane [43] and USD 1200 per metric ton of acetone [44] (estimated in 2024 U.S. dollars).

Table 1

Simulation results: mass balance and heat duty for the dehydration reaction of glucose and xylose over aluminum chloride to furans using 1,4-dioxane versus acetone as organic co-solvents. “Realistic” (closed) and “non-realistic” (open) scenarios.

Mass Balance and Heat Duty Results	1,4-dioxane “Realistic” scenario (Closed)	1,4-dioxane “Non-realistic” scenario (Open)	Acetone “Realistic” scenario (Closed)	Acetone “Non-realistic” scenario (Open)
SUGAR SOLUTION (FEED)				
Total mass flow of sugar processed (kg/h)	100	100	100	100
Glucose mass flow to reactor (kg/h)	78.3	78.3	78.3	78.3
Xylose mass flow to reactor (kg/h)	21.7	21.7	21.7	21.7
Fresh water with sugars to reactor (kg/h)	400	400	400	400
Sugars mass fraction (aq.)	0.2	0.2	0.2	0.2
Total mass flow of sugar solution (kg/h)	500	500	500	500
DEHYDRATION REACTOR				
Glucose conversion (%) - Experimental	100	100	100	100
Yield of 5-HMF (%) - Experimental	60.9	60.9	59.5	59.5
Xylose conversion (%) - Experimental	100	100	100	100
Yield of furfural (%) - Experimental	78.1	78.1	78.9	78.9
Solvent-to-water volume ratio entering the reactor	2.0	2.0	2.0	2.0
Total solvent to reactor (recirculated + fresh) (kg/h)	1638	825	658	632
Total water to reactor (recirculated + fresh) (kg/h)	792	400	416	400
Solvent/water mass ratio entering the reactor	2.1	2.1	1.6	1.6
Total mass flow to the reactor (kg/hr)	2534	1327	1176	1134
Reaction temperature (°C)	185	185	185	185
Reactor's operating pressure (kPa) - Experimental	1634	1634	2068	2068
Reactor's heat duty (MJ/hr)	1085	675	1196	1155
DISTILLATION SYSTEM				
Reflux ratio (mass basis)	1.5	1.5	1.5	1.5
Estimated total theoretical equilibrium stages required	10	10	10	10
Estimated optimal “Feed stage” location	5	5	5	5

(continued on next page)

Table 1 (continued)

Mass Balance and Heat Duty Results	1,4-dioxane "Realistic" scenario (Closed)	1,4-dioxane "Non-realistic" scenario (Open)	Acetone "Realistic" scenario (Closed)	Acetone "Non-realistic" scenario (Open)
Total mass flow to the distillation column (kg/h)	2534	1327	1176	1134
Solvent in distillate stream (kg/h)	1605	808	644	619
Water in distillate stream (kg/h)	390.6	197.2	16.0	15.3
Furfural in distillate stream (kg/h)	0.42	0.37	0.00	0.00
5-HMF in distillate stream (kg/h)	0.0	0.0	0.0	0.0
Total mass flow in distillate stream (kg/h)	1996	1006	660	635
Solvent mass fraction in distillate stream [organic solvent and water only]	0.80	0.80	0.98	0.98
Solvent mass fraction in distillate stream [Overall]	0.80	0.80	0.98	0.98
^a Recirculated distillate stream temperature (°C)	68	25	36	25
Reboiler's heat duty (MJ/h)	4308	2183	1201	1155
^b Overhead condenser's heat duty (MJ/h)	3776	1904	945	908
Top product temperature (°C)	87.9	87.9	56.4	56.4
SOLVENT & CATALYST MAKEUP				
Fixed solvent loss (%) (based on solvent to the D. C.)	2.0	2.0	2.0	2.0
Solvent entering the distillation column (kg/h)	1638	825	658	632
Solvent loss (kg/hr) [@ bottom product]	32.8	16.6	13.2	12.7
Fresh solvent makeup (kg/hr)	32.8	825	13.2	632
Dehydration catalyst makeup (AlCl₃) (kg/h)	4.8	2.4	2.5	2.4

^a In "closed" systems, the values represent an estimated temperature of the recirculated solvent, accounting for a reduction of 20 °C due to heat transfer to the surroundings. In contrast, this temperature is fixed in open systems at 25 °C (fresh solvent).

^b The thermal energy that must be "removed" at the overhead condenser to condense the vapor reaching this equilibrium stage.

3.2.5. Dehydration catalyst makeup

In the "realistic" 1,4-dioxane scenario, nearly twice the amount of catalyst makeup is required compared to its acetone counterpart (4.8 kg/hr versus 2.5 kg/hr, AlCl₃). This divergence arises from three main factors: the fixed catalyst loading defined on a concentration basis (15 mM of AlCl₃), the significantly higher volume flow rate entering the dehydration reactor for the 1,4-dioxane system (2534 kg/hr; 2.4 m³/hr) compared to the acetone system (1176 kg/hr; 1.4 m³/hr), and the

absence of a strategy for recovering the soluble aluminum chloride.

3.2.6. Heat duty and equipment size

Fig. 5 illustrates the thermal energy demand, or heat duty, required at the dehydration reactor and the reboiler of the distillation system, as well as the thermal energy that must be removed at the overhead condenser to condense the distilled product for the "realistic" scenarios of the two organic solvent systems under study. As registered in Table 1, the experimental operating pressure during the dehydration of sugars when using acetone was approximately 27 % higher than that of the 1,4-dioxane system. This result is attributed to the higher volatility of acetone, which also leads to a slightly greater thermal energy input at the dehydration reactor to compensate for the heat of vaporization (Fig. 5). The difference in operating pressure should be factored into capital expenditure estimates, as it can significantly impact equipment costs related to equipment materials, design complexity, safety features, and maintenance [45,46]. The heat duties estimated for the reboiler and overhead condenser in the "realistic" 1,4-dioxane scenario are 3.6 and 4.0 times greater, respectively, than those calculated for the corresponding acetone system. These results are attributed to the greater mass flow of materials entering the distillation column when 1,4-dioxane is used (2534 kg/h versus 1176 kg/hr). The increased flow requires more thermal energy for the components to reach the appropriate operating temperature at the overhead condenser. As shown in Fig. 4, this temperature is also higher for the azeotropic distilled product compared to the same operating condition when acetone is used. In industrial settings, the heat demand at equipment such as the dehydration reactor and the reboiler, as studied here, is typically met by heat generated from fuels combusted in power boilers [47]. Similarly, the heat duty at the overhead condenser is usually managed through cooling water circuits, cooling towers, and other refrigeration systems [48]. Based on the results, a biorefinery using 1,4-dioxane is expected to be larger than one using acetone for three main reasons: the size of the equipment in the inside battery limits (e.g., transfer pumps, reactor, and

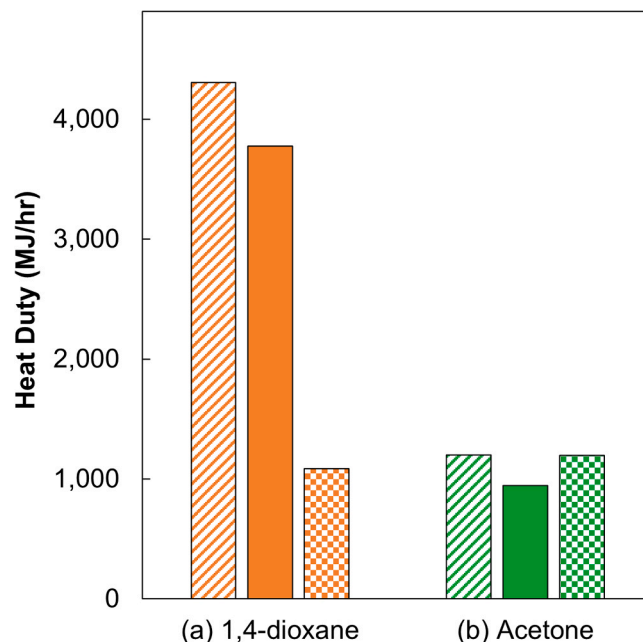


Fig. 5. ■ Reboiler, ■ Overhead condenser, and ■ Dehydration reactor heat duties for a hypothetical biorefinery processing 100 kg/h of combined glucose and xylose in a 20 wt% aqueous solution with an organic solvent-to-aqueous sugar solution volume ratio of 2–1, using (a) 1,4-dioxane and (b) acetone as organic solvents supporting the dehydration reaction of sugars. Note that the overhead condenser's heat duty corresponds to the thermal energy that needs to be removed to condense the lighter distilled product.

distillation system), which is proportional to the materials flow across the equipment (Table 1); the size of the “Heat and Power” plant; and the size of the “Utility” plant required to meet the increased heating and cooling demand, respectively. Considering the impact of equipment size and the use of fuels and chemicals on capital and operational costs, minimizing plant size and overall heat duty is essential for ensuring an economically feasible biorefinery.

3.2.7. Distillation column parameters for continuous distillation experiments

The total theoretical equilibrium stages required to recover 98 % of the solvent entering the distillation column, along with the optimal “Feed stage” location to minimize the reboiler heat duty, are determined for each system. Simulation results suggest that ten equilibrium stages, with the feed positioned above “Equilibrium stage No. 5,” are suitable for distilling 1,4-dioxane at its azeotrope concentration and nearly pure acetone in each case (Table 1). These findings informed the setup of experimental conditions for continuous distillation at the bench scale. However, due to limitations in commercially available glassware, fourteen stages were used in the experiments. Additionally, as precise instrumentation to measure the return flow to “Equilibrium stage No. 2” was unavailable, no reflux was employed during the distillation experiments.

3.3. Continuous distillation experiments

3.3.1. Continuous distillation of 1,4-dioxane from furans solution

Given the large volume of materials required for the continuous distillation study and based on the findings from the dehydration reaction experiments (Fig. 3), 300 ml of an aqueous solution containing purchased 5-HMF (6.67 wt%) and furfural (2.17 wt%) was prepared. Glucose (6.12 wt%) and xylose (0.95 wt%) were also added to the solution to simulate the presence of side products from the dehydration reaction (e.g., humin). 1,4-Dioxane was then added in a solvent-to-aqueous volume ratio of 2–1. The resulting solution was continuously transferred to the in-house-built multi-stage distillation apparatus above “Equilibrium stage No. 8” at a flow rate of 2.0 ml/min. The temperature of the liquid phase at the reboiler and the temperature of the vapor phase at “Equilibrium stage No. 2” were monitored throughout the experiment. The results revealed that thermal equilibrium was achieved after 44 minutes (Supplementary material). Upon reaching a stable state, the average reboiler temperature was 97.0 ± 0.1 °C, slightly below the setpoint temperature of 101 °C, suggesting the persistent presence of organic solvent at the reboiler. At “Equilibrium stage No. 2”, an average temperature of 86.4 ± 0.1 °C was observed, close to the azeotrope temperature for the 1,4-dioxane/water system (87.8 °C at 101.325 kPa) [21]. The volume flow of distillate was measured at 1.5 ± 0.1 ml/min. Six sample pairs (D-R1 to D-R6), comprising top and bottom products, were collected at various process times after thermal equilibrium (Supplementary material). The average 1,4-dioxane content in the distillate and bottom products is presented in Fig. 6. A mass percentage of 82.2 ± 0.1 wt% 1,4-dioxane was detected in the distilled stream, closely matching the literature-reported azeotrope concentration of 82.5 wt% [21]. However, the reboiler product still contained 13.9 ± 0.8 wt% 1,4-dioxane, indicating that additional equilibrium stages are required for the complete solvent recovery, contrary to the simulation model’s prediction.

3.3.2. Continuous distillation of acetone from furans solution

Considering the results of the sugar dehydration experiments using acetone (Fig. 3) and following the procedure outlined in the preceding section, 300 ml of a second aqueous solution containing 5-HMF (6.52 wt %), furfural (2.20 wt%), glucose (6.34 wt%) and xylose (0.92 wt%) was prepared. Acetone was added in an organic-to-aqueous volume ratio of 2–1. A flow rate of 2.0 ml/min of the acetone-containing solution was processed in the continuous distillation system. Thermal equilibrium

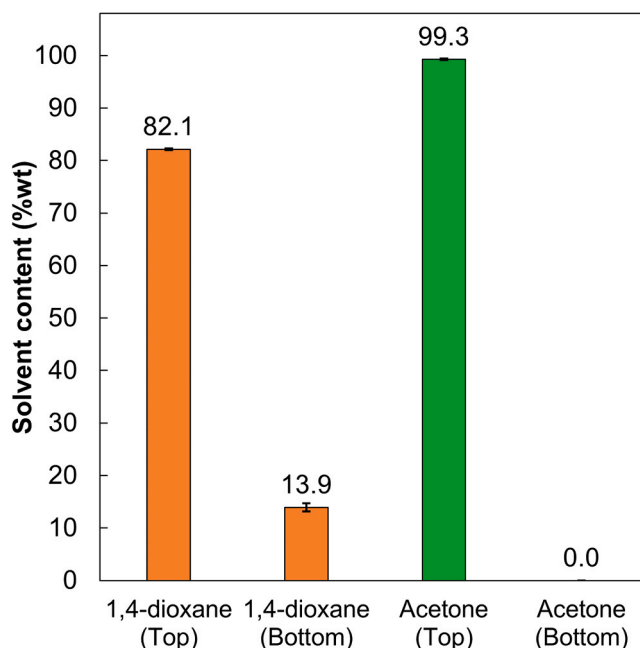


Fig. 6. Organic solvent content in the distilled and bottom products as a mass percentage for 1,4-dioxane and acetone systems.

was achieved after 16 minutes, with the reboiler at 101 ± 0.1 °C, equal to the setpoint temperature (Supplementary material), suggesting the absence of organic solvent in this stage. The temperature at “Equilibrium stage No. 2” (55.2 ± 0.1 °C) closely matched acetone’s boiling point (56 °C) [40]. The top product flow rate was measured at 1.4 ± 0.1 ml/min. The analysis of six sample pairs (A-R1 to A-R6) collected after thermal equilibrium revealed an acetone mass content of 99.3 ± 0.1 wt% in the distilled stream, with no acetone detected in the reboiler product (Fig. 6). The acetone content found in the distilled product was slightly higher than the simulation result (98 %). The presence of additional components may explain the discrepancies with simulation outcomes, as complex simultaneous interactions can occur. In contrast to the experiments involving 1,4-dioxane, fourteen equilibrium stages were sufficient for the complete recovery of high-purity acetone.

3.3.3. Distilled product from 1,4-dioxane and acetone systems

No 5-HMF was detected in the distilled products from the 1,4-dioxane or acetone experiments. Interestingly, contrary to the simulation results, furfural was found not only in the distilled 1,4-dioxane (which contained 18 wt% water), as predicted by the simulation but also in the high-purity distilled acetone, at rates of 0.25 ± 0.1 % and 0.23 ± 0.1 % of the incoming furfural entering the distillation system, respectively. The presence of furfural in the recovered solvent from the 1,4-dioxane system may be linked to the azeotrope observed for the furfural/water binary mixture, as reported in the literature at 35.5 wt% furfural and 97.6 °C [49], a phenomenon also predicted by the simulation software (34.9 wt% furfural and 98.0 °C). However, considering the high purity of the distilled acetone and the absence of an azeotrope in the acetone/furfural system [39,40], additional research is required to elucidate the underlying reasons for this observation. It is conceivable that an insufficient number of equilibrium stages may have led to the persistence of furfural in the distilled acetone. Furthermore, it is possible that other components, including acidic species and side products, influenced the relative volatility of furfural in the studied system. Finally, it is essential to recognize that the absence of humin in the model solutions used for the distillation experiments differs from real-world conditions, where the precipitation of this material may contribute to clogging in the distillation system over time, potentially posing operational challenges [11].

3.4. Industrial implications of solvent selection

In this study, the implications of using two alternative organic solvents for glucose and xylose dehydration, as well as their recyclability, are contrasted, and their significance in biorefinery design is highlighted. However, additional factors beyond the findings of this work, such as economic feasibility (solvent market price and availability), operational safety, and regulatory compliance, must be considered to fully assess the industrial applicability of acetone or 1,4-dioxane for sugar dehydration [50].

Safety is paramount in industrial operations, particularly when handling highly volatile substances. Acetone, for example, has a low flash point (-17 °C) and high volatility (vapor pressure of 24.5 kPa at 20 °C), meaning it can form ignitable vapors at low temperatures. This characteristic presents a fire hazard if not managed according to OSHA and NFPA regulations [51]. While the EPA has not established a quantitative assessment of acetone's carcinogenicity in humans, studies on inhalation exposure suggest potential mild transient neurological effects [52]. OSHA has set a permissible exposure limit (PEL) for acetone at 1000 ppm (2400 mg/m³) based on an 8-hour time-weighted average (TWA) [53]. Conversely, 1,4-dioxane poses significant health risks. In November 2024, the EPA confirmed that 1,4-dioxane presents an unreasonable risk to human health under the Toxic Substances Control Act (TSCA). Identified hazards included liver toxicity, damage to the olfactory epithelium, and an increased risk of cancer through inhalation, dermal contact, and ingestion of contaminated water [54]. OSHA has set a PEL for 1,4-dioxane at 100 ppm (360 mg/m³) on an 8-hour TWA [55].

From an environmental regulatory perspective, the EPA has not established specific nationwide effluent limitation guidelines for acetone or 1,4-dioxane. However, companies must comply with chemical-specific discharge limits outlined in National Pollutant Discharge Elimination System General Permits (NPDES). For instance, NPDES Permits MAG910000 and NHG910000, which apply to dewatering and remediation discharges in Massachusetts and New Hampshire, set effluent limitations for acetone (8.0 mg/l) and 1,4-dioxane (0.2 mg/l) [56]. These regulatory constraints are critical considerations in the design of the wastewater treatment system within the biorefinery design.

4. Conclusions

This study compares reaction performance and solvent recyclability parameters experimentally and across biorefinery simulation models for two alternative organic solvents supporting the dehydration reaction of glucose and xylose over aluminum chloride. Despite minor differences in the yield of 5-HMF and furfural, acetone outstands 1,4-dioxane when processing aqueous solutions of sugars at intermediate concentrations. The choice of acetone as the preferred solvent for this application is based on four pivotal factors: lower overall process heat demand, reduced solvent loss, decreased catalyst loss, and smaller biorefinery size. Factors that directly impact capital and operational expenditure in biorefinery operations.

CRedit authorship contribution statement

Park Sunkyu: Writing – review & editing, Supervision, Project administration, Funding acquisition, Conceptualization. **Johnson David K.:** Writing – review & editing, Supervision, Methodology, Investigation, Conceptualization. **Tiller Phoenix:** Writing – review & editing, Methodology, Data curation, Conceptualization. **Park Hyeonji:** Writing – review & editing, Methodology, Data curation, Conceptualization. **Mittal Ashutosh:** Writing – review & editing, Methodology, Investigation, Data curation, Conceptualization. **Gonzalez Ronalds:** Writing – review & editing, Supervision, Methodology, Conceptualization. **Cruz David:** Writing – review & editing, Writing – original draft, Visualization, Software, Methodology, Investigation, Formal analysis,

Data curation, Conceptualization.

Declaration of Competing Interest

The authors declare that they have no known competing financial interests or personal relationships that could have appeared to influence the work reported in this paper.

Acknowledgments

The authors gratefully acknowledge the support for this research provided by the U.S. Department of Energy through its Bioenergy Technologies Office (BETO), award number DE-EE0008498. The views expressed in this article do not necessarily represent the views of the U.S. Department of Energy or the United States.

Appendix A. Supporting information

Supplementary data associated with this article can be found in the online version at [doi:10.1016/j.jece.2025.116069](https://doi.org/10.1016/j.jece.2025.116069).

Data availability

Data will be made available on request.

References

- [1] S. Liu, G. Cheng, Industrial crops & products developments and perspectives on lignin-first biomass pretreatment for efficient enzymatic hydrolysis and isolation of lignin with minimized degradation, *Ind. Crop. Prod.* 208 (2024), <https://doi.org/10.1016/j.indcrop.2023.117926>.
- [2] S. Gupta, A.B. Gambhire, R. Jain, Conversion of carbohydrates (glucose and fructose) into 5-HMF over solid acid loaded natural zeolite (PMA/NZ) catalyst, *Mater. Lett. X* 13 (2022), <https://doi.org/10.1016/j.mblux.2021.100119>.
- [3] U.S. Department of Energy, Top. Value Added Chem. Biomass-- (2004), <https://doi.org/10.2172/15008859>.
- [4] S. Kumaravel, J.K. Alagarasan, A.K. Yadav, W. Ali, M. Lee, M.E. Khan, S.K. Ali, A. H. Bashiri, W. Zakri, K. Balu, Highly selective catalytic transfer hydrogenation of biomass derived furfural to furfural alcohol over Zr/SBA-15 catalysts, *J. Phys. Chem. Solids* 186 (2024), <https://doi.org/10.1016/j.jpcs.2023.111831>.
- [5] J. Slak, B. Pomeroy, A. Kostyniuk, M. Grlic, B. Likozar, A review of bio-refining process intensification in catalytic conversion reactions, separations and purifications of hydroxymethylfurfural (HMF) and furfural, *Chem. Eng. J.* 429 (2022), <https://doi.org/10.1016/j.cej.2021.132325>.
- [6] M.G.A. Vieira, M.A. Da Silva, L.O. Dos Santos, M.M. Beppu, Natural-based plasticizers and biopolymer films: a review, *Eur. Polym. J.* 47 (2011) 254–263, <https://doi.org/10.1016/j.eurpolymj.2010.12.011>.
- [7] J.Y. Zhu, X. Pan, Efficient sugar production from plant biomass: current status, challenges, and future directions, *Renew. Sustain. Energy Rev.* 164 (2022) 112583, <https://doi.org/10.1016/j.rser.2022.112583>.
- [8] M.S. Pino, R.M. Rodríguez-Jasso, M. Michelin, H.A. Ruiz, Enhancement and modeling of enzymatic hydrolysis on cellulose from agave bagasse hydrothermally pretreated in a horizontal bioreactor, *Carbohydr. Polym.* 211 (2019) 349–359, <https://doi.org/10.1016/j.carbpol.2019.01.111>.
- [9] F. Shiva, R.M. Climent Barba, R.K. Rodríguez-Jasso, H.A. Sukumaran, Ruiz, High-solids loading processing for an integrated lignocellulosic biorefinery: Effects of transport phenomena and rheology – A review, *Bioresour. Technol.* 351 (2022), <https://doi.org/10.1016/j.biortech.2022.127044>.
- [10] Y. Muranaka, K. Matsubara, T. Maki, S. Asano, H. Nakagawa, K. Mae, 5-hydroxymethylfurfural synthesis from monosaccharides by a biphasic reaction-extraction system using a microreactor and extractor, *ACS Omega* 5 (2020) 9384–9390, <https://doi.org/10.1021/acscomega.0c00399>.
- [11] S. Liu, Y. Zhu, Y. Liao, H. Wang, Q. Liu, L. Ma, C. Wang, Advances in understanding the humins: formation, prevention and application, *Appl. Energy Combust. Sci.* 10 (2022), <https://doi.org/10.1016/j.jaecs.2022.100062>.
- [12] J. Esteban, A.J. Vorholt, W. Leitner, An overview of the biphasic dehydration of sugars to 5-hydroxymethylfurfural and furfural: a rational selection of solvents using COSMO-RS and selection guides, *Green. Chem.* 22 (2020) 2097–2128, <https://doi.org/10.1039/c9gc04208c>.
- [13] A.I. Torres, P. Daoutidis, M. Tsapatsis, Continuous production of 5-hydroxymethylfurfural from fructose: a design case study, *Energy Environ. Sci.* 3 (2010) 1560–1572, <https://doi.org/10.1039/c0ee00082e>.
- [14] J. Granacher, R. Castro-Amoedo, F. Maréchal, Leveraging industrial biorefineries for the energy transition, *J. Clean. Prod.* 434 (2024), <https://doi.org/10.1016/j.jclepro.2023.139795>.
- [15] Y. Men, X. Du, J. Shen, L. Wang, Z. Liu, Preparation of corn starch-g-polystyrene copolymer in ionic liquid: 1-Ethyl-3-methylimidazolium acetate, *Carbohydr. Polym.* 121 (2015), <https://doi.org/10.1016/j.carbpol.2014.12.068>.

- [16] Z. Chen, L. Chen, K.S. Khoo, V.K. Gupta, M. Sharma, P.L. Show, P.S. Yap, Exploitation of lignocellulosic-based biomass biorefinery: a critical review of renewable bioresource, sustainability and economic views, *Biotechnol. Adv.* 69 (2023), <https://doi.org/10.1016/j.biotechadv.2023.108265>.
- [17] N. Aslam, A.K. Sunol, Computing all the azeotropes in refrigerant mixtures through equations of state, *Fluid Phase Equilib.* 224 (2004) 97–109, <https://doi.org/10.1016/j.fluid.2004.03.014>.
- [18] Y. He, R. Zhang, W. Song, H. Liu, J. Zhang, W. Jia, L. Peng, 1,4-Dioxane intervention enables simultaneous valorization of biomass-based C5 and C6 sugars to furfural over H β zeolite, *Chem. Eng. J.* 480 (2024) 148092, <https://doi.org/10.1016/j.cej.2023.148092>.
- [19] Y. Kim, A. Mittal, D.J. Robichaud, H.M. Pilath, B.D. Etz, P.C. St. John, D. K. Johnson, S. Kim, Prediction of hydroxymethylfurfural yield in glucose conversion through investigation of lewis acid and organic solvent effects, *ACS Catal.* 10 (2020) 14707–14721, <https://doi.org/10.1021/acscatal.0c04245>.
- [20] M. Kato, H. Konishi, M. Hirata, Apparatus for measurement of isobaric dew and bubble points and vapor-liquid equilibria methanol-water and water-dioxane systems, *J. Chem. Eng. Data* 15 (1970) 501–505, <https://doi.org/10.1021/je60047a022>.
- [21] M. Hichri, R. Besbes, Z. Trabelsi, N. Ouerfelli, I. Khattech, Isobaric vapour-liquid phase diagram and excess properties for the binary system 1,4-dioxane + water at 298.15 K, 318.15 K and 338.15 K, *Phys. Chem. Liq.* 52 (2014) 373–387, <https://doi.org/10.1080/00319104.2013.833618>.
- [22] M. Lafranconi, J. Anderson, R. Budinsky, L. Corey, N. Forsberg, J. Klapacz, M. J. LeBaron, An integrated assessment of the 1,4-dioxane cancer mode of action and threshold response in rodents, *Regul. Toxicol. Pharmacol.* 142 (2023), <https://doi.org/10.1016/j.yrtph.2023.105428>.
- [23] S. Bakshi, U. Sarkar, R. Villa, D. Basu, D. Sengupta, Conversion of biomass to biofuels through sugar platform: a review of enzymatic hydrolysis highlighting the trade-off between product and substrate inhibitions, *Sustain. Energy Technol. Assess.* 55 (2023) 102963, <https://doi.org/10.1016/j.seta.2022.102963>.
- [24] H. Park, D. Cruz, P. Tiller, D.K. Johnson, A. Mittal, H. Jameel, R. Venditti, S. Park, Effect of ash in paper sludge on enzymatic hydrolysis, *Biomass-- Bioenergy* 165 (2022) 106567, <https://doi.org/10.1016/j.biombioe.2022.106567>.
- [25] X. Zhang, B.B. Hewetson, N.S. Mosier, Kinetics of maleic acid and aluminum chloride catalyzed dehydration and degradation of glucose, *Energy Fuels* 29 (2015) 2387–2393, <https://doi.org/10.1021/ef502461s>.
- [26] A. Mittal, H.M. Pilath, D.K. Johnson, Direct conversion of biomass carbohydrates to platform chemicals: 5-hydroxymethylfurfural (HMF) and furfural, *Energy Fuels* 34 (2020) 3284–3293, <https://doi.org/10.1021/acs.energyfuels.9b04047>.
- [27] D. Saang'onyo, S. Parkin, F.T. Ladipo, Effect of ancillary (aminomethyl)phenolate ligand on efficacy of aluminum-catalyzed glucose dehydration to 5-hydroxymethylfurfural, *Polyhedron* 149 (2018) 153–162, <https://doi.org/10.1016/j.poly.2018.03.035>.
- [28] V. Choudhary, A.B. Pinar, S.I. Sandler, D.G. Vlachos, R.F. Lobo, Xylose isomerization to xylulose and its dehydration to furfural in aqueous media, *ACS Catal.* 1 (2011) 1724–1728, <https://doi.org/10.1021/cs200461t>.
- [29] J.B. Sluiter, R.O. Ruiz, C.J. Scarlata, A.D. Sluiter, D.W. Templeton, Compositional analysis of lignocellulosic feedstocks. 1. Review and description of methods, *J. Agric. Food Chem.* 58 (2010) 9043–9053, <https://doi.org/10.1021/jf1008023>.
- [30] Y. Román-Lesfkhov, C.J. Barrett, Z.Y. Liu, J.A. Dumesic, Production of dimethylfuran for liquid fuels from biomass-derived carbohydrates, *Nature* 447 (2007) 982–986, <https://doi.org/10.1038/nature05923>.
- [31] H. Zhu, Y. Zhang, X. Guo, Y. Cheng, L. Wang, X. Li, Efficient one-pot production of 5-hydroxymethylfurfural from glucose in an acetone-water solvent, *Ind. Eng. Chem. Res.* 61 (2022) 5661–5671, <https://doi.org/10.1021/acs.iecr.2c00502>.
- [32] T. Tongtummachat, A. Jaree, N. Akkarawatkhosith, Continuous hydrothermal furfural production from xylose in a microreactor with dual-acid catalysts, *RSC Adv.* 12 (2022) 23366–23378, <https://doi.org/10.1039/d2ra03609f>.
- [33] F. Gu, Y. Hou, Salt effects on the isobaric vapor-liquid equilibrium for four binary systems, *J. Chem. Eng. Data* 45 (2000) 467–470, <https://doi.org/10.1021/je990215s>.
- [34] V. Larnaudie, M.D. Ferrari, C. Lareo, Techno-economic analysis of a liquid hot water pretreated switchgrass biorefinery: effect of solids loading and enzyme dosage on enzymatic hydrolysis, *Biomass-- Bioenergy* 130 (2019) 105394, <https://doi.org/10.1016/j.biombioe.2019.105394>.
- [35] S.V. Obydenkova, P.D. Kouris, D.M.J. Smeulders, M.D. Boot, Y. van der Meer, Evaluation of environmental and economic hotspots and value creation in multi-product lignocellulosic biorefinery, *Biomass-- Bioenergy* 159 (2022) 106394, <https://doi.org/10.1016/j.biombioe.2022.106394>.
- [36] H. Renon, J.M. Prausnitz, Local compositions in thermodynamic excess functions for liquid mixtures, *AIChE J.* 14 (1968) 135–144, <https://doi.org/10.1002/aic.690140124>.
- [37] M.A. Kougioumtzis, A. Marianou, K. Atsonios, C. Michailof, N. Nikolopoulos, N. Koukouzas, K. Triantafyllidis, A. Lappas, E. Kakaras, Production of 5-HMF from cellulosic biomass: experimental results and integrated process simulation, *Waste Biomass-- Valoriz.* 9 (2018) 2433–2445, <https://doi.org/10.1007/s12649-018-0267-0>.
- [38] J. Poleđnová, I. Wichterle, Vapour-liquid equilibrium in the acetone-water system at 101.325kPa, *Fluid Phase Equilib.* 17 (1984) 115–121, [https://doi.org/10.1016/0378-3812\(84\)80015-1](https://doi.org/10.1016/0378-3812(84)80015-1).
- [39] Y. Ma, J. Gao, M. Li, Z. Zhu, Y. Wang, Isobaric vapour-liquid equilibrium measurements and extractive distillation process for the azeotrope of (N,N-dimethylisopropylamine + acetone), *J. Chem. Thermodyn.* 122 (2018) 154–161, <https://doi.org/10.1016/j.jct.2018.03.019>.
- [40] M.G. Myles, R.E. Wingard, Calculating activity coefficients, *Ind. Eng. Chem.* 53 (1961) 219–222, <https://doi.org/10.1021/ie50615a029>.
- [41] W. Li, H.T. Lu, M.S. Doblin, A. Bacic, G.W. Stevens, K.A. Mumford, A solvent loss study for the application of solvent extraction processes in the pharmaceutical industry, *Chem. Eng. Sci.* 250 (2022) 117400, <https://doi.org/10.1016/j.ces.2021.117400>.
- [42] B. Nemeth, P. Lang, L. Hegely, Optimisation of solvent recovery in two batch distillation columns of different size, *J. Clean. Prod.* 275 (2020) 122746, <https://doi.org/10.1016/j.jclepro.2020.122746>.
- [43] W. Li, A. Ghosh, D. Bbosa, R. Brown, M.M. Wright, Comparative techno-economic, uncertainty and life cycle analysis of lignocellulosic biomass solvent liquefaction and sugar fermentation to ethanol, *ACS Sustain. Chem. Eng.* 6 (2018) 16515–16524, <https://doi.org/10.1021/acssuschemeng.8b03622>.
- [44] G. Dalle Ave, T.A. Adams, Techno-economic comparison of Acetone-Butanol-Ethanol fermentation using various extractants, *Energy Convers. Manag.* 156 (2018) 288–300, <https://doi.org/10.1016/j.enconman.2017.11.020>.
- [45] J.C. Atuonwu, S.A. Tassou, Model-based energy performance analysis of high pressure processing systems, *Innov. Food Sci. Emerg. Technol.* 47 (2018) 214–224, <https://doi.org/10.1016/j.ifset.2018.02.017>.
- [46] W.L. Luyben, Capital cost of compressors for conceptual design, *Chem. Eng. Process. - Process. Intensif.* 126 (2018) 206–209, <https://doi.org/10.1016/j.cep.2018.01.020>.
- [47] M. Skibrowski, Synthesis and design methods for energy-efficient distillation processes, *Curr. Opin. Chem. Eng.* 42 (2023), <https://doi.org/10.1016/j.coche.2023.100985>.
- [48] N. Jourdan, M. Kanniche, T. Neveux, O. Potier, Numerical simulation of hydrodynamics in wet cooling tower packings, *Int. J. Refrig.* 153 (2023) 194–204, <https://doi.org/10.1016/j.ijrefrig.2023.05.022>.
- [49] L.C. Nhien, N.V.D. Long, S. Kim, M. Lee, Techno-economic assessment of hybrid extraction and distillation processes for furfural production from lignocellulosic biomass, *Biotechnol. Biofuels* 10 (2017) 1–12, <https://doi.org/10.1186/s13068-017-0767-3>.
- [50] M.S. Wagh, S. S. P.C. Nath, A. Chakraborty, R. Amrit, B. Mishra, A.K. Mishra, Y. K. Mohanta, Valorisation of agro-industrial wastes: circular bioeconomy and biorefinery process – a sustainable symphony, *Process Saf. Environ. Prot.* 183 (2024) 708–725, <https://doi.org/10.1016/j.psep.2024.01.055>.
- [51] Sigma-Aldrich, Material safety data sheet - Acetone, (2024). (<https://www.sigmaaldrich.com>).
- [52] U.S. Environmental Protection Agency (EPA), Toxicological review of acetone (CAS No. 67-64-1), 2003. (<https://iris.epa.gov>).
- [53] U.S. Occupational Safety and Health Administration, OSHA Occupational chemical database - Acetone, (2024). (<https://www.osha.gov/>).
- [54] U.S. Environmental Protection Agency, Unreasonable risk determination for 1,4-dioxane, 2024. (<https://www.epa.gov/>).
- [55] U.S. Occupational Safety and Health Administration, OSHA Occupational chemical database - 1,4-dioxane, (2024). (<https://www.osha.gov/>).
- [56] U.S. Environmental Protection Agency, NPDES Permit No. MAG910000 and NHG910000, 2017. (<https://www.epa.gov/>).